Carbohydrate Polymers 267 (2021) 118190

Contents lists available at ScienceDirect

Carbohydrate Polymers

journal homepage: www.elsevier.com/locate/carbpol

Cryotropic gel-forming capacity of alfalfa (*Medicago sativa* L.) and fenugreek (*Trigonella foenum graecum*) seed galactomannans

Thierry Hellebois [a,b], Claire Gaiani [b,e], Jennyfer Fortuin [a,c], Alexander Shaplov [d], Christos Soukoulis [a,*]

[a] Environmental Research and Innovation (ERIN) Department, Luxembourg Institute of Science and Technology (LIST), 5 avenue des Hauts Fourneaux, Esch-sur-Alzette L4362, Luxembourg
[b] Université de Lorraine, LIBio, Nancy, France
[c] Trier University of Applied Sciences, Department of Food Technology, Schneidershof, 54293 Trier, Germany
[d] Materials Research and Technology (MRT) Department, Luxembourg Institute of Science and Technology (LIST), 5 avenue des Hauts Fourneaux, Esch-sur-Alzette, L4362, Luxembourg
[e] Institut Universitaire de France (IUF), France

ARTICLE INFO

Keywords:
Cryogel
Cryostructuration
Dynamic rheology
Microstructure
Galactomannan
Synergism

ABSTRACT

Cryotropic gelation is one of the most common approaches to design novel hydrogels with multifaceted technological and biological functionalities. In the present paper, we studied the ability of highly galactosyl-substituted galactomannans, i.e. fenugreek and alfalfa gum, to form physically crosslinked hydrogels via cryogenic processing. Cycling of the galactomannan solutions (0.25 to 4% wt) from 25 to −20 to 25 °C induced the physical crosslinking of the galactomannan chains leading to the formation of different cryogel structures, i.e. filamentous aggregates ($c^* < c < 1\%$), cellular-like gel networks ($1 \leq c < 4\%$) or a homogeneously swollen gel ($c \geq 4\%$), depending on the total biopolymer content. Alfalfa gum-based cryogels exhibited higher elasticity and stiffness, better uniformity of the structure and a lower macropore size than their fenugreek counterparts. The physical blending of alfalfa or fenugreek gum with locust bean gum (2% total biopolymer) led to the reinforcement of the mechanical properties of the cryogels without significantly altering their microstructural aspects.

1. Introduction

The term cryogel refers to the polymeric structurates formed via cryogenic processing (Lozinsky, 2018). Cryotropic gelation process occurs via a liquid-solid phase transition of the solvent (e.g. water) at temperatures below the freezing point of the solvent, but well above the glass transition temperature (T_g) of the polymeric solution (Lozinsky, 2018). The cryo-concentration of the continuous (bulk) aqueous phase increases the solute(s) partition in the unfrozen micro-phase, favoring the non-covalent (e.g. hydrogen bonds or hydrophobic) intermolecular polymer interactions that eventually lead to the formation of a hydrophilic macroporous (varying pore size from 0.1 to 10 μm) or supermacroporous (pore size up to a few hundred micrometers) polymeric structure (Lozinsky, 2018; Saylan & Denizli, 2019).

Depending on their properties, i.e., the average size of the pores and capillaries, mechanical strength and resilience, biocompatibility and biodegradability, cryogels can be employed for biomedical, material composites, biotechnological, environmental and food technology applications (Ertürk & Mattiasson, 2014; Kirsebom et al., 2009; Nakagawa & Nishimoto, 2011; Saylan & Denizli, 2019). In food applications, cryogels may be used for either texturizing purposes (i.e., preserving the structural integrity and textural quality of mostly frozen food products) or controlled release of bioactive compounds (Lazaridou & Biliaderis, 2007; Nakagawa & Nishimoto, 2011; Patmore et al., 2003; Sun et al., 2021). To date, food macromolecules, such as polysaccharides (e.g. galactomannans, cereal β-glucans, xanthan, sodium alginate, starch) and proteins (e.g. whey proteins, albumin, gelatin), have been successfully used as single or *co*-polymer cryostructurants (Balaji et al., 2019; Doyle et al., 2006; Giannouli & Morris, 2003; Lazaridou & Biliaderis, 2007; Lozinsky et al., 2000b; Zou & Budtova, 2020). Besides the inherent cryotropic gel-forming capacity of the food biopolymers, parameters such as the biopolymer thermodynamic compatibility, biopolymer

* Corresponding author.
E-mail address: christos.soukoulis@list.lu (C. Soukoulis).

https://doi.org/10.1016/j.carbpol.2021.118190
Received 7 March 2021; Received in revised form 25 April 2021; Accepted 7 May 2021
Available online 12 May 2021

solvent affinity, cryoscopic properties of the solutes, presence and amount of solute impurities, and the cryogenic processing conditions (e.g. ice nucleation and crystallization dynamics, occurrence of ice recrystallization during frozen storage, number of freeze-thaw cycles, rate of ice crystals fusion etc.) are significant determinants of the structural and mechanical characteristics of the final cryogel (Baudron et al., 2019; Giannouli & Morris, 2003; Kirsebom et al., 2009; Lozinsky, 2018; Lozinsky et al., 2000b; Saylan & Denizli, 2019; Tanaka et al., 1998).

Galactomannans are heterogeneous polysaccharides comprising a β − (1 → 4) D-mannose backbone branched with α − (1 → 6) linked D-galactose monomeric units (Kontogiorgos, 2019). It is well-accepted that the mannose-to-galactose ratio (M/G) defines the techno-functionality of galactomannans, i.e. cold-water swelling ability, thickening, gelling, film-forming and cryogelation properties (Kontogiorgos, 2019). The most-studied galactomannans include fenugreek (M/G ~ 1), guar (M/G ~ 2), tara (M/G ~ 3) and locust bean gum (M/G ~ 4) (Dea et al., 1977; Gillet et al., 2017; Kontogiorgos, 2019). More recently, the rheological and structure conformational profile of alfalfa gum (*Medicago sativa* L. M/G ~ 1) has been studied (Hellebois, Soukoulis, et al., 2021). Natively or enzymatically galactose depleted galactomannans (>M/G ~ 3) have displayed very good cryogelation properties (Doyle et al., 2006; Lozinsky et al., 2000a, 2000b; Tanaka et al., 1998). Tanaka et al., (1998), while investigating the cryogel forming capacity of guar, tara and locust bean gum (LBG) under varying cryo-processing conditions, demonstrated that only LBG could assure prominent cryotropic gelation, which was inextricably associated with the number of freeze-thaw cycles (maximized after 3 consecutive cycles) and the cooling rate (the higher the cooling rate, the higher the hydrogel elasticity G′ achieved). In the subsequent study of Lozinsky et al., (2000b), it was evidenced that the cryotropic gelation of LBG occurred via the establishment of multiple hydrogen bonds between the hydroxyl groups of the polygalactomannan chains. The LBG concentration regime (dilute, semi-dilute or concentrated) was proven to modulate the structural features of the cryogels, i.e. soft spongy, cellular and non-spongy homogenous hydrogels, respectively (Lozinsky et al., 2000b). The impact of galactose content, molecular weight and co-solutes (viz fructose, glucose, sorbitol and sucrose) on the structural and mechanical properties of LBG and debranched (galactose depleted) guar gum was studied by Doyle et al. (2006). According to their findings, the increase in the M/G ratio of the galactomannan led to cryogels with improved mechanical properties. On the other hand, the binding affinity of the sugar co-solutes to the galactomannan (via hydrogen bond interactions) was the most probable mechanism explaining its cryotropic gelation activity.

Although, highly galactosyl substituted galactomannans (M/G ~ 1) have been reported for their good hydrogel forming properties via chemo-enzymatic oxidation (Galante et al., 2018), there are no existing literature data pointing out their capacity to undergo cryotropic gel (physical) formation. According to recent preliminary findings (Soukoulis & Hellebois, 2020), both fenugreek and alfalfa galactomannans exhibited a weak hydrogel forming ability under freezing – thawing conditions. It is hypothesized that the large number of galactosyl moieties present in galactomannans with M/G ratio close to unity favors the hydrogen bond intra– and intermolecular bridging of the galactomannan polymer chains under cryoconcentration conditions, leading to the formation of cryogels of diversified microstructural aspects. To address this research question, alfalfa (AAG) and fenugreek (FG) galactomannan solutions (0.25 to 4% wt) were subjected to different cryogenic processing conditions, and the obtained cryogels were characterized by means of oscillatory thermo-rheological, differential scanning calorimetry and microstructural analyses. In addition, the cryostructuring synergism between AAG or FG with LBG was experimentally justified.

2. Materials and methods

2.1. Extraction and specification of the galactomannans

Fenugreek (Planète au Naturel, France) and alfalfa (Food to Live, New York, USA) seeds were purchased from the local market. Galactomannans were extracted, isolated and purified from the fenugreek and alfalfa seed meal according to the procedure described by Hellebois, Soukoulis, et al. (2021). In addition, locust bean gum (Sigma Aldrich, Leuven, Belgium) was reconstituted in hot water (at 80 °C under magnetic stirring for 1 h), cooled down at room temperature and purified according to the aforementioned procedure. All galactomannan gums were stored in a desiccator cabinet (Nalgene, ThermoFisher, Belgium) at ambient temperature and 0% relative humidity to prevent water uptake during storage. The detailed proximate and osidic composition of fenugreek (M/G = 1.09) and alfalfa (M/G = 1.18) galactomannans was determined as detailed in Hellebois, Soukoulis, et al. (2021) and it is given in Suppl. Table 1.

2.2. In-situ cryogel formation and rheological characterization

Galactomannan solutions (1 to 4% wt) were prepared by dispersing the appropriate amount of gum into MilliQ water at 50 °C under turbulent mechanical stirring. All galactomannan dispersions were heated at 80 °C for 30 min, cooled down to 25 °C, balanced with water to their initial weight (to avoid any discrepancies due to water evaporation) and kept under agitation overnight to allow full hydration. A small amount of sodium azide (0.02% wt) was added as a bacteriostatic.

Cryogel formation and characterization was conducted in situ in a controlled stress oscillatory rheometer (MCR 302, Anton Paar, Graz, Austria) using a profiled plate – plate geometry (25 mm). A small amount (ca. 750 mg) of galactomannan solution was transferred onto the measuring plate and the gap was adjusted to 1 mm (the gap expansion due to ice formation was less than 1% for all tests). The galactomannan systems were pre-sheared at 25 °C for 1 min at 30 s^{-1} and allowed to rest for 5 min. Cryogel formation was conducted in five consecutive freeze–thaw cycles according to the following protocol: 1) cooling from 25 to −20 °C at the rate of 5 °C min^{-1}, 2) isothermal hold at −20 °C for 15 min, 3) heating from −20 to 25 °C at the rate of 5 °C min^{-1} and 4) isothermal hold at 25 °C for 5 min. The viscoelastic moduli G′ and G″ (in Pa) were recorded throughout the entire in situ cryogelation process.

The initial galactomannan solutions and the cryogels obtained at the end of the freeze–thaw procedure were characterized by means of frequency and amplitude sweep oscillatory rheological tests, as detailed in Hellebois, Soukoulis, et al. (2021). The dynamic rheological spectra were analyzed using RheoCompass software (Anton Paar, Graz, Austria).

2.3. DSC measurements

A TA instruments (Discovery DSC 250, New Castle, USA) Differential Scanning Calorimeter (DSC) was used for carrying out all thermal analysis experiments. Aliquots of individual FG, AAG, LBG or binary (1:1 blends of FG or AAG gum with LBG) galactomannan solutions (2% wt) were weighed into aluminum pans (ca. 30 mg) ensuring maximal contact with the pan surface. The pans were hermetically sealed and the following thermal scanning protocol, corresponding to one complete freeze–thaw cycle, was employed: 1) isothermal hold at 25 °C for 10 min, 2) cooling to −30 °C at 5 °C min^{-1}, 3) isothermal hold at −30 °C for 15 min, 4) heating to 25 °C at 5 °C min^{-1} and 5) isothermal hold at 25 °C for 10 min. Following five freeze–thaw cycles, the in situ formed cryogel was heated from 25 to 100 °C at 2 °C min^{-1} in order to evaluate its melting behavior. An aluminum pan containing 30 mg of deionised (MilliQ water) was used as reference for calculating the enthalpy of fusion (ΔH) of pure water. The TA Universal Analysis software (TA instruments, New Castle, USA), was used to calculate the onset and

midpoint temperatures as well as the enthalpies of the detected endothermic (ice fusion) peaks.

2.4. Confocal Laser Scanning Microscopy (CLSM) assessment of the cryogels

Cryogels (0.25–4% wt biopolymer) based on either individual (FG, AAG, LBG) or binary galactomannan blends (1:1 blend of LBG with FG or AAG, 2% wt total solids) were prepared as aforementioned. The galactomannan solutions were non covalently stained with 40 μL mL^{-1} of 0.1% wt of Calcofluor solution, degassed via centrifugation at 3000*g* for 5 min and aliquots of ca. 300 mg were carefully transferred into eight well Nunc Lab-Tek II chamber microscope slides. To promote cryotropic gelation, the microscope slides were transferred into a freezing chamber at −20 °C and subjected into five freeze–thaw cycles, as described in Section 2.2.

The microstructure of the cryogels was assessed at ambient temperature using Confocal Laser Scanning Microscopy (CLSM, LSM 880 with Airy scan, Zeiss, Jena, Germany) equipped with 10× and 20× objective lenses. The used fluorophore was excited at 405 nm and the emitted fluorescence signal was detected at 407–471 nm. The images obtained were analyzed using ImageJ software to characterize the macroporous network as described schematically in Suppl. Fig. 1.

2.5. Statistical analyses

The normal distribution of the data was verified by means of the Shapiro-Wilk test and Q-Q plot representation. In addition, the equality of variance among the variables was verified using the Levene test. To determine the significance of AAG and FG concentration on the physicochemical and rheological properties, one-way ANOVA was performed using Origin 2019b software (OriginLab Inc., USA). Tukey's multiple range test was used to separate means of data when significant differences ($p < 0.05$) were detected.

3. Results and discussion

3.1. Effect of freezing time and freeze-thaw cycling on cryogels elasticity

Aside from the chemical composition and concentration of the cryotropic gel-forming biopolymer, the cryogenic processing conditions, i.e. freeze-thaw rate, number of freeze-thaw cycles and duration of the frozen storage are important drivers of the mechanical and morphological properties of the cryo-structured matrix (Lozinsky et al., 2000b; Tanaka et al., 1998). The thermal history of the biopolymer solutions affects the ability of the polymer chains to undergo intermolecular association, which in turn influences not only the mechanical properties of the final hydrogels but also their thermo-reversible behavior. In the case of LBG cryogels, Lozinsky et al. (2000b) demonstrated that decreasing the frozen storage temperature and thawing rate results in rigid hydrogels with a high melting temperature point. Preliminary investigation of the impact of freezing and thawing rates (0.5, 1, 5 and 10 °C min^{-1}) on the elastic modulus of single-cycled 2% wt AAG and FG solutions (data not shown) revealed only minor changes (less than 10%) in the G′ values at 1 Hz, with the highest values being achieved at 1 and 5 °C min^{-1}. Therefore, the dynamic rheological and thermal analyses were conducted at the rate of 5 °C min^{-1}. On the other hand, the duration of frozen storage time and the number of freeze-thaw cycles had a significant impact ($p < 0.001$) on the G′ values of the FG and AAG cryogels obtained (Fig. 1). As seen in Fig. 1a, the G′ of the obtained cryogels after a single freeze-thaw cycle increased sharply during the first 30 min of tempering at −20 °C, reaching a pseudo-equilibrium after approx. 120 min of frozen storage. It has been well-established that the dynamics of ice crystallization, i.e. the kinetics of ice nucleation, the cryo-concentration of the unfrozen phase and the ripening of ice crystals, directly influence the porogens (ice crystals) and therefore, they define the mechanical and structural profile of the cryogels. Based on our preliminary observations (Suppl. Fig. 2), the impact of frozen storage time (15 and 120 min at −30 °C) on the enthalpies of the ice fusion peaks of the DSC thermographs, only had a minor influence on the total amount of ice formed, and this may explain the negligible impact of the frozen storage time on the development of storage modulus after 1 h.

On the other hand, the number of freeze-thaw cycles had a decisive effect on the structural and mechanical reinforcement of the cryogels, as seen in Fig. 1B. The cryogel elasticity was developed progressively, reaching a pseudo-equilibrium after 6–8 freeze thaw cycles. In agreement with the findings of Tanaka et al. (1998), the storage modulus of LBG (2% wt) was maximized and stabilized after three freeze-thaw cycles (Suppl. Fig. 3), which indicates the better ability of LBG to undergo non-covalent interchain association under freeze-thawing conditions. Based on the aforementioned observations, the rheological and thermal investigation of all galactomannan aqueous systems was conducted adopting five freeze–thaw cycling measuring protocols at 5 °C min^{-1}.

3.2. Effect of galactomannans concentration on their cryogel forming capacity

The cryogel forming capacity of biopolymers is influenced in a manner roughly equivalent to the conventional gelation (at positive temperatures) (Lozinsky & Okay, 2014). In the case of conventional gelation, the biopolymer precursors (polysaccharides or proteins) need to exceed a minimal (critical) concentration (CCG) in order to promote

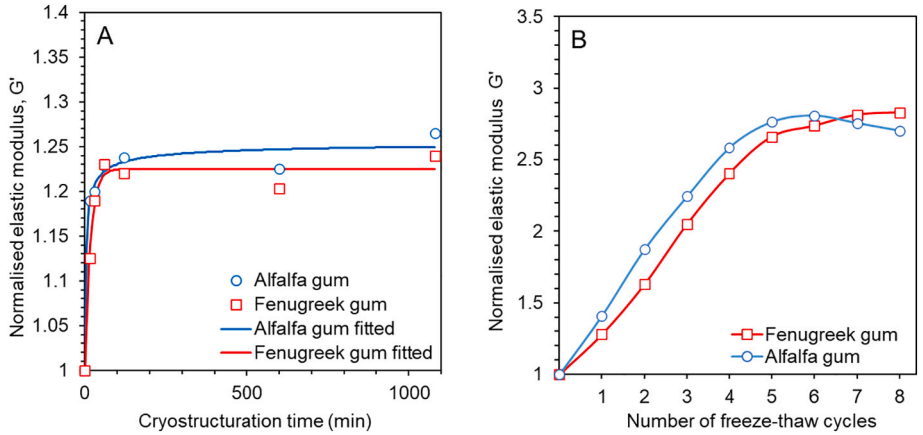

Fig. 1. Impact of frozen storage time (single freeze–thaw cryotropic induced gelation) (A) and number of freeze-thaw cycles on the normalised (to the galactomannan solution) elastic modulus G′ measured at 25 °C (strain 0.5%, $f = 1$ Hz) (B).

the formation of elastically active crosslinks (physical or covalent) that lead to the development of a three-dimensional hydrogel structure (Hellebois, Gaiani, et al., 2021; Nicolai, 2019). Although the CCG is inherent to the biopolymer chemical structure and molecular properties, it has been well-documented that cryogel formation can be achieved at significantly low precursor concentrations (Lozinsky & Okay, 2014). For example, insoluble sponge-like cryogels were obtained at concentrations as low as 0.2, 0.3 and 1–2% wt for xanthan, locust bean gum and oat β-glucans, respectively (Giannouli & Morris, 2003; Lazaridou & Biliaderis, 2004; Lozinsky et al., 2000b).

In Fig. 2 is illustrated the impact of the galactomannan type and concentration on the elastic modulus of the cryogels obtained. As clearly depicted, the responsiveness of the mechanical strength of the cryogels was progressively increased with galactomannan concentration, with the alfalfa-based ones to exert the steepest increase. On the other hand, when the G′ values of the cryogels were normalised to those of the initial galactomannan solutions, the total galactomannan content was inversely associated with the percentual changes in the G′ values.

In addition, the tanδ dependence on biopolymer concentration, which is indicative of the interconnectivity of the elastically active macropores, remained unclear (Table 1). Therefore, it is postulated that the increase in the galactomannan content does not elicit a de facto improvement of the cryogel stiffness, which is ascribed to the net contribution of the solid (i.e., interconnected biopolymer chain network) and viscous (i.e., unbound water present in the macroporous cavities) structure elements to the overall viscoelastic behavior of the obtained cryogels. As illustrated in the CLSM micrographs (Fig. 2), for galactomannan concentrations below 0.5% wt, cryogels exhibiting an aggregated filamentous microstructure with a very limited number of interconnected macropores were obtained. Therefore, the freeze-thaw processing of AAG and FG solutions at the dilute to semi-dilute transitive state ($c^* = 0.31$ for AAG (Hellebois, Soukoulis, et al., 2021) and $c^* = 0.39$ for FG (Suppl. Fig. 4), respectively) resulted in very weak cryogels, which is consistent with the observations of Lozinsky et al.

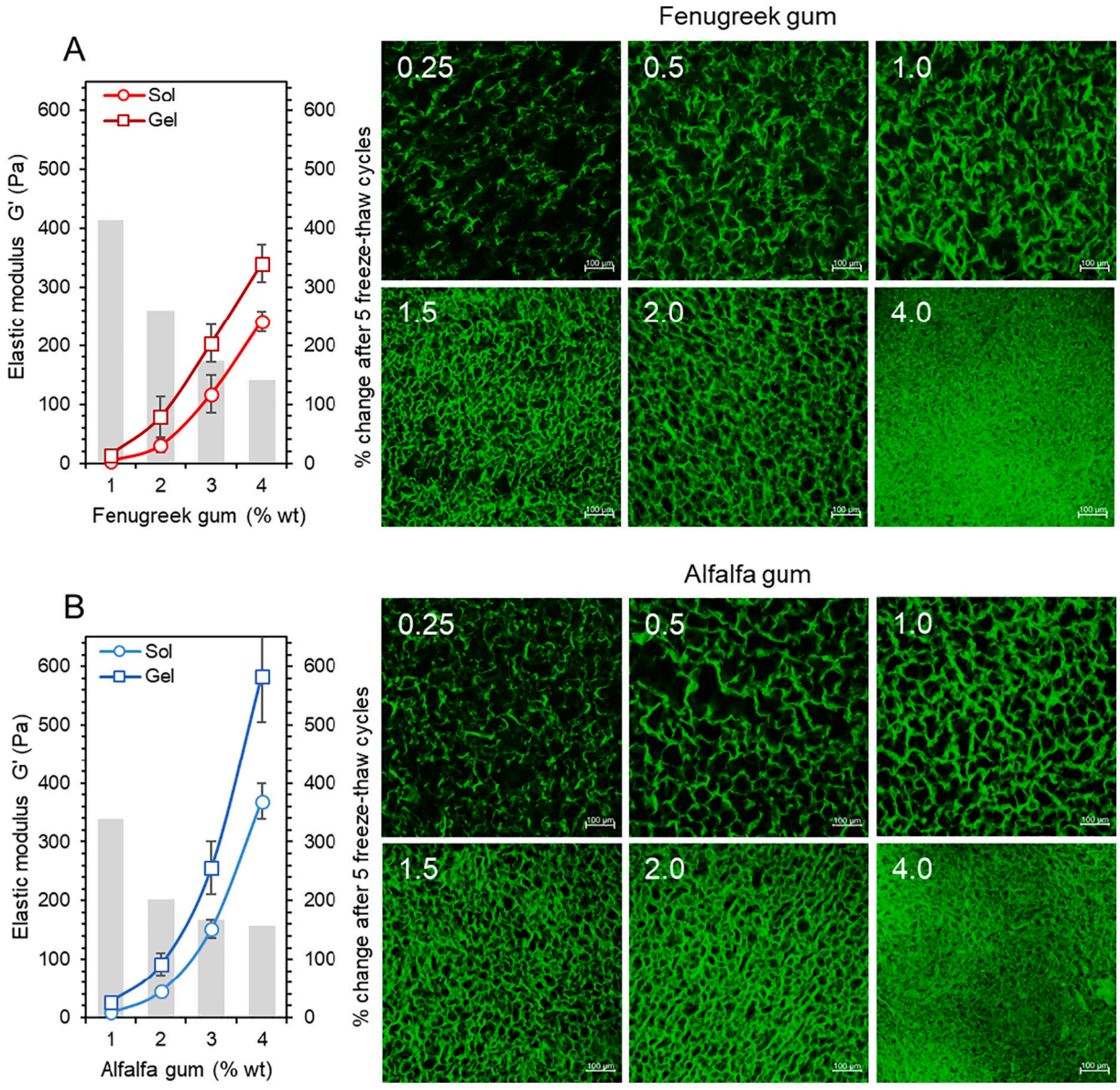

Fig. 2. Effect of fenugreek (A) and alfalfa (B) galactomannan concentration (% wt) on the mechanical properties of the initial aqueous solutions (sol) and the cryogels (gel) obtained after five freeze-thaw cycles (25 to −20 to 25 °C at 5 °C min-1, 15 min isothermal hold at −20 °C) and CLSM-assisted assessment of their microstructural characteristics (0.25 to 4% wt) at 25 °C. Galactomannan-rich microdomains (visualized in green color) were stained with Calcofluor white. Magnification: 10×, scale bar = 100 μm.

Table 1
Effect of galactomannan concentration (1–4% wt) on the rheological properties of the initial aqueous solutions and the cryogels obtained after five freeze-thaw cycles (25 to −20 to 25 °C at 5 °C min^{-1}, 15 min isothermal hold at −20 °C). Different letters between the concentrations (lowercase) or state (uppercase) indicate a significant difference ($p < 0.05$) according to Tukey's post hoc means comparison test. n.d.: not detected.

State	Gum concentration	Strain sweeps					Frequency sweeps			
		G'_{LVE}	G''_{LVE}	Yield stress, τ_y	Flow point, τ_f	G'_f	Flow transition index	Crossover frequency f_c	Slope G′-f	Stiffness tan δ
	(%)	(Pa)	(Pa)	(Pa)	(Pa)	(Pa)		(Hz)		
Fenugreek gum										
Sol	1	$3.2^{a,A}$	$3.3^{a,A}$	$1.2^{a,A}$	n.d.	n.d.	–	0.90^{b}	$1.00^{b,B}$	$0.95^{c,B}$
	2	$30.3^{b,A}$	$22.3^{b,A}$	$14.9^{b,A}$	$33.3^{a,A}$	$20.1^{a,A}$	–	0.48^{ab}	$0.80^{ab,B}$	$0.80^{bc,B}$
	3	$120.2^{c,A}$	$72.6^{c,A}$	$53.6^{c,A}$	$156.2^{b,A}$	$63.1^{b,A}$	–	0.19^{a}	$0.70^{ab,B}$	$0.63^{ab,B}$
	4	$260.4^{d,A}$	$135.0^{d,A}$	$116.3^{d,A}$	$332.1^{c,A}$	$110.7^{c,A}$	–	0.08^{a}	$0.60^{a,BC}$	$0.53^{a,B}$
Gel	1	$14.5^{a,B}$	$5.1^{a,A}$	$8.7^{a,B}$	9.2^{a}	6.7^{a}	1.05^{a}	n.d.	$0.20^{a,A}$	$0.47^{a,A}$
	2	$75.4^{b,B}$	$28.7^{b,AB}$	$41.2^{b,AB}$	$70.1^{b,AB}$	$31.5^{b,AB}$	1.70^{b}	n.d.	$0.24^{a,A}$	$0.44^{a,A}$
	3	$206.1^{c,B}$	$86.4^{c,A}$	$77.9^{c,AB}$	$232.4^{c,AB}$	$84.6^{c,AB}$	2.98^{d}	n.d.	$0.39^{a,A}$	$0.47^{a,AB}$
	4	$361.0^{d,B}$	$157.6^{d,B}$	$160.9^{d,B}$	$324.4^{d,A}$	$98.0^{c,A}$	2.02^{c}	n.d.	$0.41^{a,AB}$	$0.44^{a,AB}$
Alfalfa gum										
Sol	1	$7.9^{a,A}$	$6.3^{a,A}$	$6.1^{a,A}$	$8.0^{a,A}$	$5.8^{a,A}$	–	0.48^{a}	$0.78^{d,B}$	$0.80^{c,B}$
	2	$46.0^{b,A}$	$27.8^{b,A}$	$25.7^{b,A}$	$61.3^{b,A}$	$23.4^{b,A}$	–	0.14^{b}	$0.64^{c,B}$	$0.60^{c,B}$
	3	$158.6^{c,A}$	$71.5^{c,A}$	$70.0^{c,A}$	$196.4^{c,A}$	$60.1^{c,A}$	–	0.03^{c}	$0.50^{b,B}$	$0.46^{b,AB}$
	4	$394.7^{d,A}$	$140.8^{d,A}$	$157.5^{d,A}$	$415.8^{d,A}$	$128.7^{d,B}$	–	n.d.	$0.39^{a,B}$	$0.36^{a,AB}$
Gel	1	$24.5^{a,B}$	$7.3^{a,A}$	$9.5^{a,A}$	$13.4,^{a,B}$	$7.9^{a,A}$	1.41^{a}	n.d.	$0.14^{a,A}$	$0.28^{a,A}$
	2	$89.6^{b,B}$	$32.7^{b,A}$	$57.7^{b,B}$	$117.9^{b,B}$	$36.4^{b,AB}$	2.04^{b}	n.d.	$0.23^{ab,A}$	$0.36^{a,A}$
	3	$263.7^{c,B}$	$86.7^{c,B}$	$126.7^{c,B}$	$273.2^{c,A}$	$90.5^{c,B}$	2.16^{b}	n.d.	$0.27^{b,A}$	$0.34^{a,A}$
	4	$605.6^{d,B}$	$176.3^{d,B}$	$205.1^{d,B}$	$431.6^{d,A}$	$125.2^{c,AB}$	2.10^{b}	n.d.	$0.27^{b,A}$	$0.29^{a,A}$

(2000b). As the galactomannan solutions departed from the critical coil overlap concentration (c*), the ability of the biopolymer chains to form stable physical interconnections was substantially improved, as depicted by the formation of cellular macroporous structures (Fig. 2). The increase in the measured G′ values appeared to be inversely associated to the c* of the galactomannans i.e., the lower the c* value of the solution the higher the gel firmness achieved. It has been previously shown that galactomannans of M/G > 3 can form stable hydrogel networks via multiple inter- and intramolecular hydrogen bonds between the hydroxyl groups of the polymeric chains (Lozinsky et al., 2000b; Tanaka et al., 1998). Due to the limited number of the galactose depleted mannan sequences in AAG and FG, it is presumed that the stabilization of the cryogel network is governed by hydrogen bond crosslinking in the junction zones of the polygalactomannans. To confirm this hypothesis, the galactomannans were mixed with a chaotropic compound (i.e. urea) at varying concentrations (0.25 to 3 M) and subjected to the same cryogenic processing conditions. The presence of urea resulted in a decisive suppression of the cryostructuring capacity of both galactomannans as confirmed by the sequential development of the normalised G′ values (Fig. 3). In addition, the CLSM visualization of the microstructure of the galactomannan aqueous systems containing 3 M of urea indicated an almost complete loss of the galactomannans' ability to create cellular-like gel networks (Fig. 3). It should be noted that the cryogenically processed galactomannan solutions containing urea did not exhibit any self-standing gel behavior as the urea-free counterparts. The ability of chaotropic substances (ionic or non-ionic) to hamper the cryogel forming capacity of polymers due to the steric hindering of hydrogen bonding and the decrease in the partitioning of the cryogel forming polymer in the unfrozen liquid microphase (UFLMP) has been reported by Kolosova et al. (2018).

Image processing of the cryogel micrographs confirmed that the increase in the galactomannan total solids (from 0.25 to 4% wt) induced a progressive decrease in the macropore mean area occupancy (porosity) and Feret's mean diameter values (Fig. 4A, B). In order to have a better insight into the uniformity of the macropores, the pore area cumulative curves were constructed (Fig. 4C, D) and a 3-parameter sigmoidal model (Eq. (1)) was fitted:

$$y = 100 \cdot \frac{a}{1 + \left(\frac{x}{b}\right)^{n}} \quad (1)$$

where a is an asymptomatic value (100%), b denotes the inflection point that represents the area at 50% of the cumulative distribution function, and n is a constant associated with the rate of change (slope) of the distribution.

As depicted in Fig. 4C, D, the hydrogels obtained from the cryogenically processed AAG solutions exhibited a more uniform macroporous structure than their FG hydrogel counterparts. Despite the fact that the increase in the galactomannan total solids was associated with a progressive increase in the pore uniformity, the responsiveness of the inflection points to the biopolymer content was different among the tested galactomannans. In general, AAG appeared to have a better structuring ability at lower concentrations (i.e., 1.5% wt) compared to FG (≥2% wt). However, the microstructural differences between AAG and FG cryogels were diminished at 4% wt.

The rheological characteristics of the galactomannan cryogels at 25 °C, calculated by the amplitude and frequency sweep spectra (Suppl. Fig. 5), are given in Table 1. By increasing the galactomannan total solids, a progressive increase in the limiting value of the LVE region was observed in terms of the storage modulus G'_{LVE} and yield stress (Table 1). This implies that the deformability of the cryogels is reciprocally associated with the interconnectivity and the average size of the macropores. Thus, cryogels characterized by high compactness and uniformity of their percolated polymeric structure are able to withstand higher external shear forces without undergoing irreversible (plastic) deformation (Mezger, 2014). Except for the 1% wt FG solution, all systems underwent a solid-to-liquid phase transition, with the flow point values (τ_f) increasing proportionally to the galactomannan content. Given that the flow transition index values were close to unity and the loss factor, i.e. tanδ >0.1, it can be postulated that all cryogels exhibited a brittle soft gel-like behavior (Mezger, 2014). The flow transition index values were adversely correlated ($r = -0.938$ and -0.981, for AAG and FG, respectively) to the Feret diameters indicating the presence of large macropores, which increased the sensitivity of the cryogels to shear induced structural collapse.

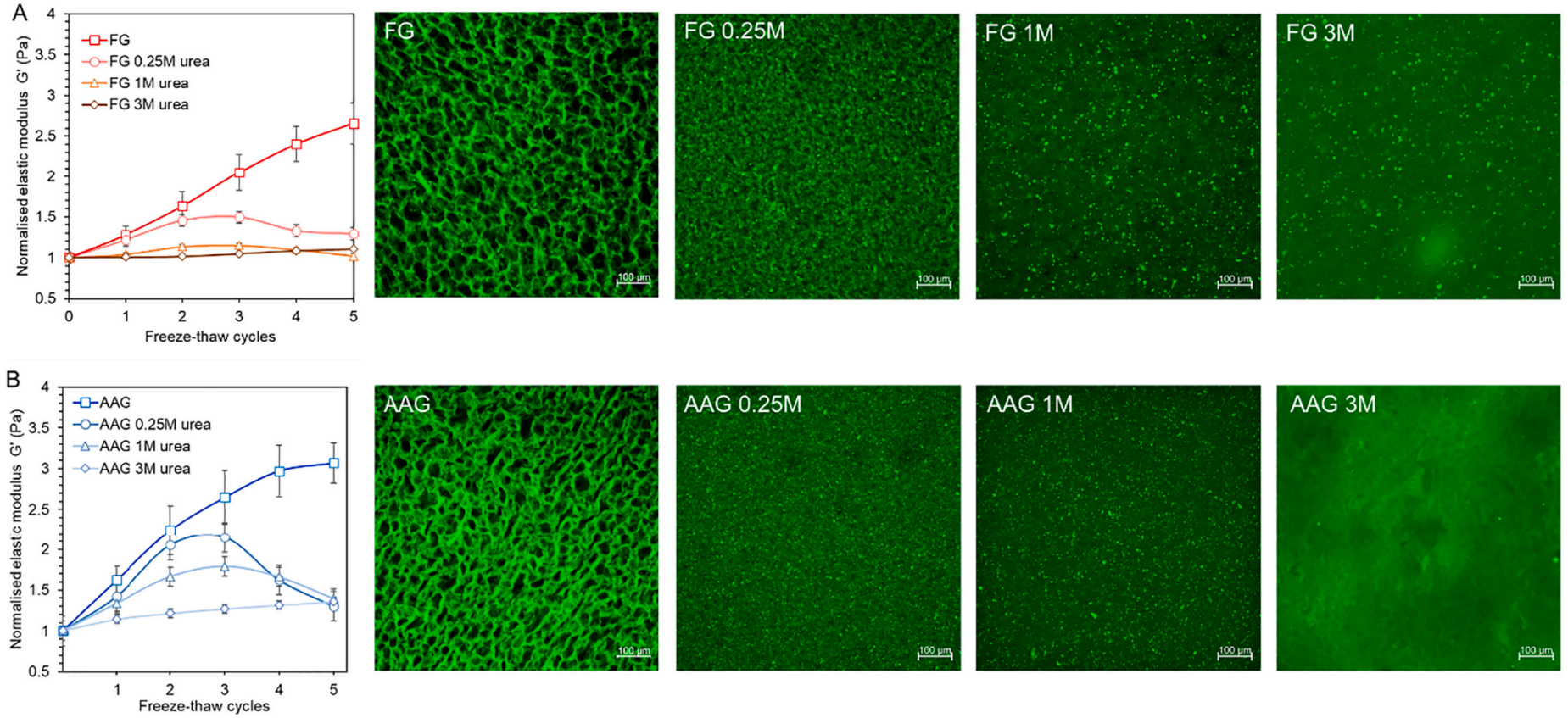

Fig. 3. Development of the elastic modulus G′ (normalised values) measured at 25 °C of 2% AAG (A) and FG (B) (strain 0.5%, $f = 1$ Hz) and CLSM micrographs of the AAG and FG cryogels in the absence or presence of urea (0.25 – 3 M). Galactomannan-rich microdomains (visualized in green color) were stained with Calcofluor white. Magnification: 10×, scale bar = 100 µm.

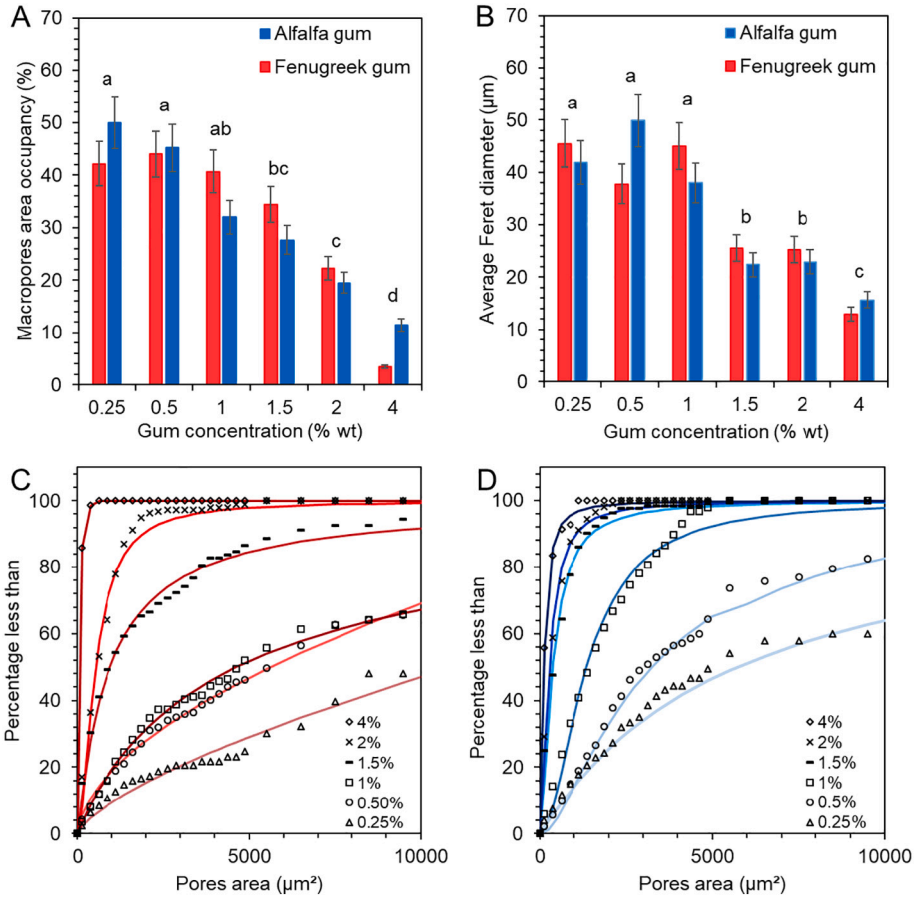

Fig. 4. Dimensional properties of the macroporous cryogel systems as influenced by the galactomannan type and concentration. Different letters between the concentrations indicate a significant difference ($p < 0.05$) according to Tukey's post hoc means comparison test.

3.3. Synergism of alfalfa and fenugreek gum with locust bean gum

The physical blending of biopolymers is considered as the most facile method to engineer their techno-functional properties (Imre & Pukánszky, 2013). In most of the cases, food biopolymers are thermodynamically incompatible, which signifies that they show partial miscibility, i.e. their blends are characterized by at least two distinct microdomains rich in one biopolymer or another (Tolstoguzov, 2008). The threshold of the biopolymer miscibility is described by the excluded volume effect, which is influenced by their structure conformational properties e.g. molecular weight, degree of branching flexibility of the chains, vibrational, rotational and hydration properties (Tolstoguzov, 2008). In order to investigate the thermodynamic compatibility between highly substituted and galactose-depleted galactomannans, binary aqueous systems comprising AAG or FG and LBG were prepared and processed cryogenically as mentioned above. In the unfrozen (solution) state, both AAG and FG were partially miscible with LBG, as indicated by the reduction in the G′ values of the binary galactomannan systems (Suppl. Fig. 6). As a general trend, AAG presented a better thermodynamic compatibility with LBG than FG. Given that all galactomannans were characterized by almost equivalent surface charge densities (ca. -1 mV), it is considered unlikely that their immiscibility stems from electrostatic repulsive forces between the polymers. On the other hand, LBG was characterized by a significantly lower molecular weight ($M_w = 1.29 \times 10^6$ Da) and higher hydrodynamic diameter values ($d_h = 170$ nm) than FG ($M_w = 1.76 \times 10^6$ Da, $d_h = 76$ nm) and AAG ($M_w = 2.0 \times 10^6$ Da, $d_h = 98$ nm). Furthermore, it has previously been shown that the solvent (water) affinity of the galactomannans tested decreases in the following order: FG > AAG > LBG (Hellebois, Soukoulis, et al., 2021). Therefore, it is assumed that the co-existence of LBG with AAG or FG creates spatial occupancy limitations under semi-dilute biopolymer solution conditions. The lower thermodynamic compatibility observed between LBG and FG can be ascribed to the self-association (via the galactose depleted mannose sequences) and lower water affinity of the former, forcing FG to undergo hydrogen bond interchain interactions and the molecules of FG to interact via hydrogel bond in the far-excluded volume region (Doyle et al., 2009; Tolstoguzov, 2008).

Cryogenic processing of the binary galactomannan solutions (2% wt) led to synergistic effects relating to the formation of elastically active non-covalent crosslinks (Fig. 5). The absence of monotonic dependence of the storage modulus on the AAG:LBG and FG:LBG mass fraction has been also observed in other binary biopolymer systems such as amylose/amylopectin (Lozinsky et al., 2000a). In general, AAG was more efficient in cooperative cryotropic gel formation with LBG than FG. Yet, similarities were observed in the way that highly substituted galactomannans influenced the cryogelation capacity of LBG. In both cases, the cryogel elasticity (Fig. 5) and mechanical strength against external shearing forces (Table 2) were maximized at the AAG- or FG- to-LBG ratio of 0.25. It should be noted that the physical blending of LBG with AAG or FG endowed the binary cryogels a brittle (flow behavior index close to unity) true gel-like (tanδ close to 0.1, G′ - *f* slope values close to 0) characteristics, a behavior that was not detected in the individual galactomannan cryogels.

As illustrated in Fig. 6, the departure of the cryogel systems from the LVE regime coincided with a progressive increase in the viscous modulus (G″), ending in a well-defined peak close to the flow transition point. It is well-known that this behavior occurs in hydrogels where the applied shear forces do not result in sudden structural collapse but most likely the gel structure is disrupted via the formation of microfissures, propagated with increasing shear stress (Mezger, 2014). The blending of

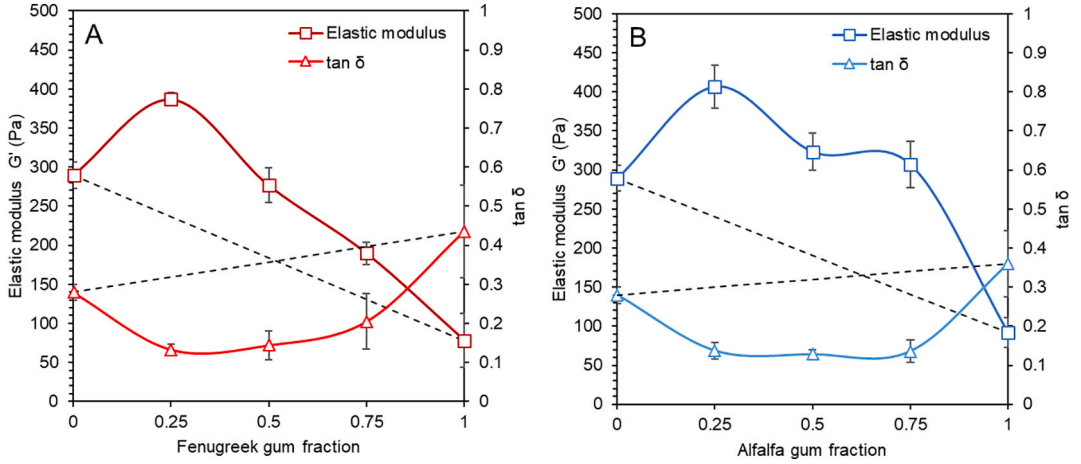

Fig. 5. Effect of FG (A) and AAG (B) fraction in a 2% wt LBG binary blends on the stiffness (tanδ) and elastic modulus ($f = 1$ Hz, strain = 0.5%, 25 °C) of cryogel after 5 freeze-thaw cycles. The dashed lines represent the theorical values of an ideal blending behavior of the two biopolymers.

Table 2
Effect of FG and AAG binary blend with LBG (2% wt total solids) on the rheological properties of the initial aqueous solutions and the cryogels obtained after five freeze-thaw cycles (25 to −20 to 25 °C at 5 °C min^{-1}, 15 min isothermal hold at −20 °C). Different letters between the ratio (lowercase) or state (uppercase) indicate a significant difference ($p < 0.05$) according to Tukey's post hoc means comparison test. n.d.: not detected.

State	Gum fraction	Strain sweeps					Frequency sweeps			
		G'_{LVE}	G''_{LVE}	Yield stress, τ_y	Flow point, τ_f	G'_f	Flow transition index	Crossover frequency f_c	Slope G'-f	Stiffness tanδ
		(Pa)	(Pa)	(Pa)	(Pa)	(Pa)		(Hz)		
	LBG:FG	Fenugreek gum								
	1:0	$147.4^{c,A}$	$89.5^{c,A}$	$55.36^{c,A}$	$186.2^{c,A}$	$73.16^{d,A}$	–	0.22^{a}	$0.46^{a,B}$	$0.66^{a,A}$
	3:1	$97.2^{bc,A}$	$72.0^{bc,BC}$	$48.9^{bc,A}$	$100.7^{b,A}$	$64.9^{cd,A}$	–	0.38^{a}	$0.66^{b,B}$	$0.78^{a,A}$
Sol	1:1	$65.5^{ab,A}$	$49.6^{ab,A}$	$41.3^{abc,A}$	$67.6^{ab,A}$	$44.9^{bc,A}$	–	0.40^{a}	$0.66^{b,B}$	$0.80^{a,A}$
	1:3	$50.0^{ab,A}$	$35.3^{a,A}$	$23.3^{ab,A}$	$53.9^{a,A}$	$31.2^{ab,A}$	–	0.39^{a}	$0.69^{bc,B}$	$0.79^{a,A}$
	0:1	$30.3^{a,A}$	$22.3^{a,A}$	$14.9^{a,A}$	$33.3^{a,A}$	$20.1^{a,A}$	–	0.48^{a}	$0.80^{c,B}$	$0.80^{a,A}$
	1:0	$283.1^{c,B}$	$87.8^{b,A}$	$150.7^{bc,B}$	$282.3^{c,B}$	$115.7^{cd,B}$	1.87^{a}	n.d.	$0.13^{a,A}$	$0.28^{ab,B}$
	3:1	$365.3^{d,B}$	$51.4^{a,AB}$	$214.8^{c,B}$	$320.1^{c,B}$	$140.1^{d,B}$	1.49^{a}	n.d.	$0.06^{a,A}$	$0.13^{a,B}$
Gel	1:1	$255.4^{c,B}$	$39.1^{a,A}$	$159.8^{bc,B}$	$251.4^{c,B}$	$97.8^{bc,B}$	1.57^{a}	n.d.	$0.08^{a,A}$	$0.14^{a,B}$
	1:3	$193.6^{b,B}$	$41.6^{a,A}$	$117.5^{ab,B}$	$164.2^{b,B}$	$70.7^{b,B}$	1.39^{a}	n.d.	$0.12^{a,A}$	$0.21^{a,B}$
	0:1	$75.4^{a,B}$	$28.7^{a,AB}$	$41.2^{a,AB}$	$70.1^{a,AB}$	$31.5^{a,AB}$	1.70^{a}	n.d.	$0.24^{b,A}$	$0.44^{c,B}$
	LBG:AAG	Alfalfa gum								
	1:0	$147.4^{d,A}$	$89.5^{e,A}$	$55.3^{c,A}$	$186.2^{c,A}$	$73.16^{d,A}$	–	0.22^{ab}	$0.46^{a,B}$	$0.66^{ab,B}$
	3:1	$111.3^{c,A}$	$78.1^{d,B}$	$55.9^{c,A}$	$119.5^{b,A}$	$69.5^{d,A}$	–	0.28b	$0.63^{c,B}$	$0.71^{b,B}$
Sol	1:1	$85.1^{bc,A}$	$58.1^{c,AB}$	$47.4^{bc,A}$	$98.0^{ab,A}$	$51.4^{c,A}$	–	0.25^{ab}	$0.62^{c,B}$	$0.70^{b,B}$
	1:3	$81.3^{b,A}$	$44.4^{b,A}$	$42.0^{b,A}$	$101.8^{ab,A}$	$36.7^{b,A}$	–	0.06a	$0.55^{ab,B}$	$0.56^{a,B}$
	0:1	$46^{a,A}$	$27.8^{a,A}$	$25.7^{a,A}$	$61.3^{a,A}$	$23.4^{a,B}$	–	0.14^{ab}	$0.64^{c,B}$	$0.60^{ab,B}$
	1:0	$283.1^{b,B}$	$87.8^{c,A}$	$150.7^{c,B}$	$282.3^{c,B}$	$115.7^{c,B}$	1.87^{b}	n.d.	$0.13^{a,A}$	$0.28^{bc,A}$
	3:1	$387.7^{c,B}$	$57.0^{b,A}$	$220.0^{d,B}$	$268.5^{c,B}$	$127.5^{c,B}$	1.22^{a}	n.d.	$0.07^{a,A}$	$0.14^{ab,A}$
Gel	1:1	$305.1^{b,B}$	$41.2^{ab,A}$	$156.^{9c,B}$	$237.3^{bc,B}$	$118.9^{c,B}$	1.51^{ab}	n.d.	$0.06^{a,A}$	$0.13^{a,A}$
	1:3	$280.6^{b,B}$	$41.1^{ab,A}$	$97.3^{bc,B}$	$160.7^{ab,B}$	$70.4^{b,B}$	1.6^{5ab}	n.d.	$0.08^{a,A}$	$0.14^{a,A}$
	0:1	$89.6^{a,B}$	$32.7^{a,A}$	$57.7^{a,B}$	$117.9^{a,B}$	$36.4^{a,AB}$	2.04^{c}	n.d.	$0.23^{b,A}$	$0.36^{c,A}$

LBG with AAG or FG intensified that phenomenon, which indicates that the rupture of the internal superstructure is associated with the relative molecular motion of the polymeric moieties that are not fixated into the gel network, such as free polymer molecules, flexible side chains or polymeric chain ends, long network bridges, etc. The highly substituted galactomannan-to-LBG ratio did not significantly alter the pattern of the viscous modulus curves.

In order to exclude any indirect effects of the biopolymer physical blending on the phase transition of water, the initial individual and binary galactomannan solutions were analyzed cycle-per-cycle by means of DSC (Fig. 7). As expected, neither the galactomannan type nor the cryogenic processing significantly influenced the colligative properties of the biopolymer solutions, with the unfrozen water content (ranging from 5.8 to 9.5% wt) and the onset ice fusion temperature points (ranging from −2.46 to −2.01 °C). It was previously shown that polysaccharides do not impact the colligative properties (freezing point depression and ice fusion enthalpies) and the ice nucleation phenomena in sugar aqueous solutions (Hagiwara & Hartel, 1996; Regand & Goff, 2002). On the other hand, in the case of the FG solution, a progressive increase was observed in the amount of unfrozen water (from 6.7 to 9.5% wt), the onset (from −2.17 to −1.92 °C) and midpoint (from 3.85 to 5.68 °C) ice fusion temperature points as a function of the freeze-thaw cycling. Although the mechanistic pathway remains unclear, it is hypothesized that FG, due it having a higher water affinity than AAG and LBG (Doyle et al., 2009; Gillet et al., 2017; Hellebois, Soukoulis, et al., 2021), can interact easily via intermolecular hydrogen bonds with water molecules and therefore, requires less water for crystallization and more energy in order to overcome the polymer – water intermolecular attractions shifting the melting temperature points to higher values (Hartel, 2001). Interestingly, when FG was blended with LBG in equal amounts, no remarkable modification of the ice fusion endothermic peaks was detected suggesting that LBG is the governing polymer in

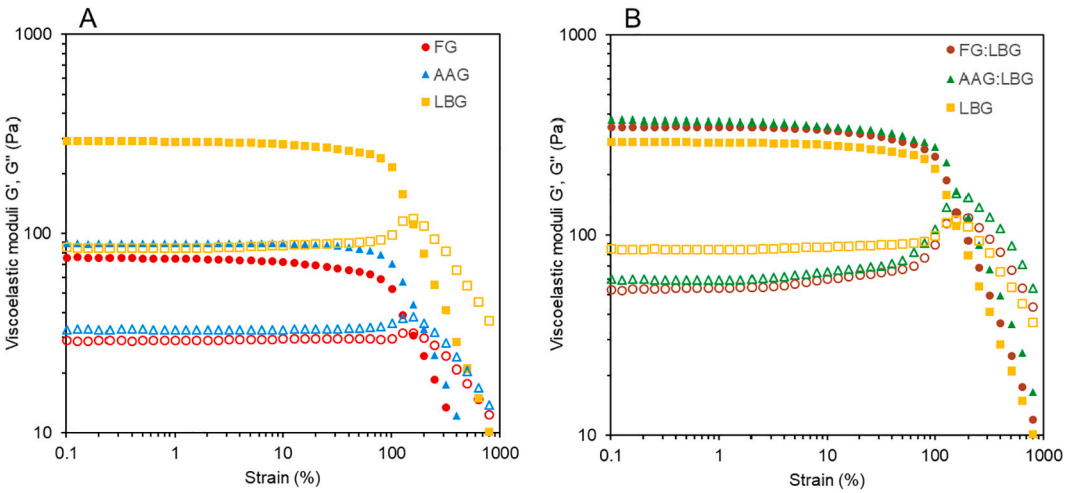

FIG. 6. Amplitude ($f = 1$ Hz) sweep rheological spectra of 2% wt galactomannan cryogel (A) and FG or AAG 1:3 LBG blend (B) 2% wt cryogels. Closed symbols = Storage modulus, G′ and open symbols = Loss modulus, G″.

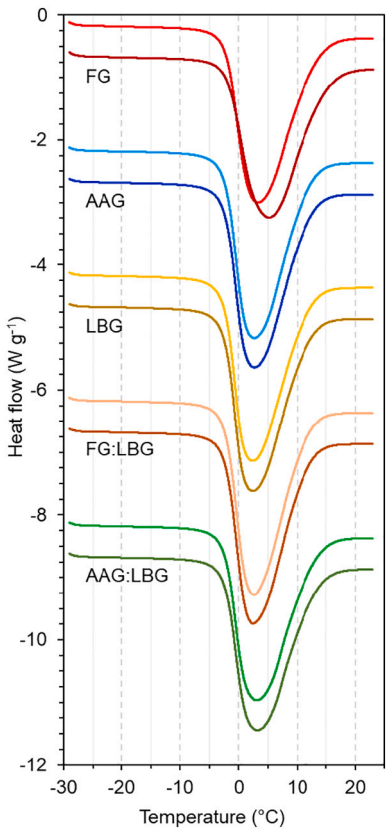

Fig. 7. DSC thermographs illustrating the melting profile of FG, AAG, LBG and binary blends (1:1) of AAG or FG with LBG after the first and fifth cycle. For emphasis reasons, AAG, LBG, FG:LBG and AAG:LBG were lowered by 2.0, 4.0, 6.0 and 8.0 W g^{-1}, respectively. In addition, the fifth cycle value of each gum was lowered by 0.5 W g^{-1} compared to the first cycle melting profile.

water-polymer interactions during crystallization. In addition, the heat was ramped up to 100 °C after the fifth freeze thaw cycle did not reveal cryogel melting. This corroborates with the findings of Dea et al. (1977) who reported that galactomannan cryogels show no real melting point but disintegrate on heating to give a suspension of gel particles.

As illustrated in the CLSM micrographs of individual and binary galactomannan cryogel systems (Fig. 8), LBG cryogels exhibited a fine-stranded cellular-like microstructure. The image processing of the cryogel micrographs revealed that the AAG- and FG-based cryogels had a significantly greater macropores wall thickness than their LBG counterparts. This most probably stems from the ability of LBG to undergo self-assembly via hydrophobic polymer – polymer interactions between the galactose-depleted (smooth regions) mannan sequences, which favor the formation of tight-zone junctions (Dea et al., 1977). Blending the LBG with either AAG or FG resulted in quite fine and uniform gel networks with the average Feret's diameter of the macropores ranging from 22 to 27 μm, which was slightly lower than the individual LBG cryogels, i.e. 34 μm (Fig. 8).

In a mechanistic context, it is assumed that the synergistic interactions between highly substituted galactomannans and LBG emanate from the ability of the polymer chains to undergo non-covalent bridging via either hydrogen bonds or hydrophobic interactions between the mannan-rich sequences (Doyle et al., 2006). Although hydrogen bond bridging with LBG molecules appears to be the same between AAG and FG, the occurrence of hydrophobic interactions is inextricably associated with the mannose-to-galactose ratio of the galactomannan (M/G = 1.09 and 1.18 for FG and AAG, respectively) and the polymer solvation affinity to water. According to the experimental findings, FG exhibited a higher water affinity ($k_{Huggins} = 0.47$) than AAG ($k_{Huggins} = 0.85$), which suggests the preferential ability of AAG polymer chains to undergo polymer – polymer than polymer – water interactions. Due to the partial immiscibility of the galactomannan species observed, it is assumed that under cryotropic processing conditions, the intra- and interchain associated galactomannan aggregate species (AAG, FG and LBG) interact via non-covalent (hydrogen bonding and hydrophobic) supramolecular forces resulting in a mechanically reinforced gel structure. The higher hydrophobic character and lower critical coil overlap concentration of AAG appears that concomitantly favor the non-covalent bridging of its self-aggregated clusters with their LBG counterparts, which in turn explains the higher cryogel forming capacity of the AAG:LBG systems as compared to the FG:LBG ones.

The CLSM micrographs did not allow us to confirm whether the unlike galactomannans were fully or partially miscible at gel state conditions. Considering that the cryogenic processing resulted in superconcentrated galactomannan solutions, i.e. 21 to 34% wt total biopolymer solids, it is rather unlikely that phase separation occurred due to volume exclusion effects (Tolstoguzov, 2008). This may also explain the high uniformity and interconnectivity of the cryogel superstructure elements. The labelling of the individual polymers via antibody or covalently bound fluorophores is required to confirm the thermodynamic compatibility of LBG with AAG or FG under

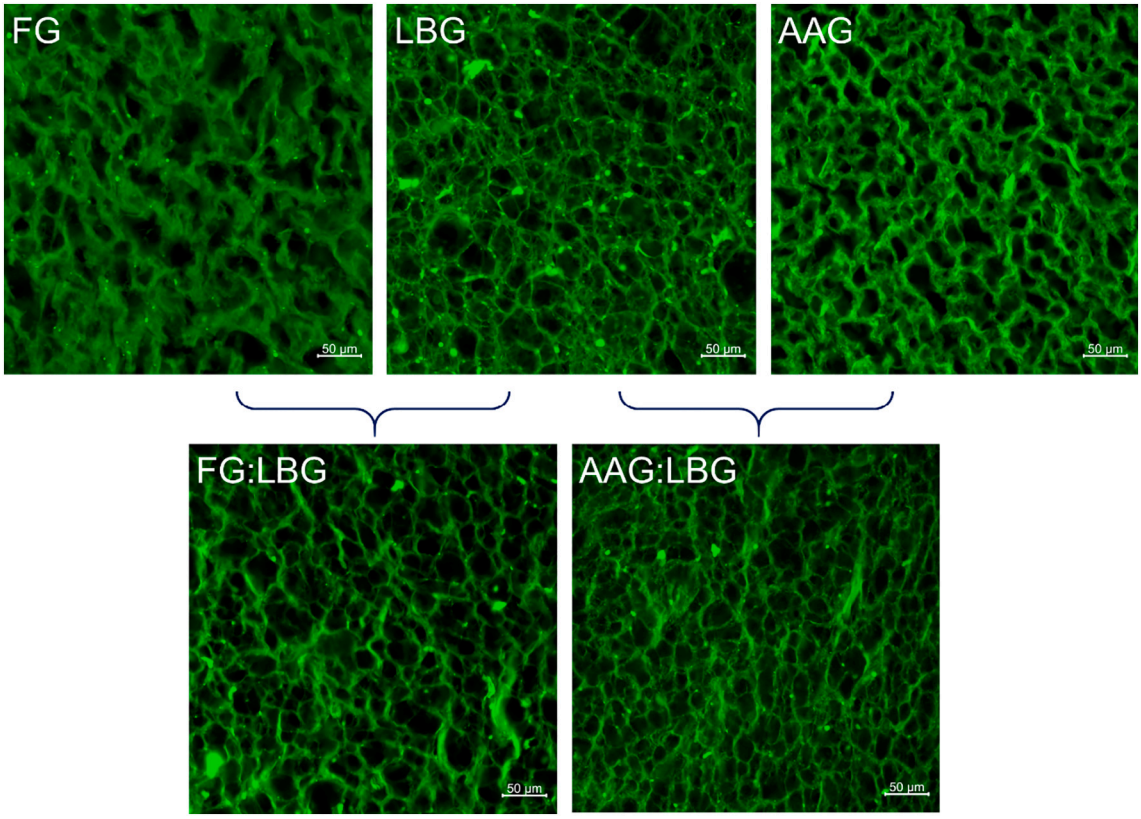

Fig. 8. CLSM-assisted assessment (at ambient temperature) of the microstructural characteristics of cryogels prepared by individual (FG, LBG and AAG) or binary galactomannan blends (FG:LBG 1:1, AAG:LBG 1:1; total biopolymer content was 2% wt). Galactomannan rich microdomains (visualized in green color) were stained with Calcofluor white. Magnification: 20×, scale bar = 50 µm.

cryoconcentration conditions.

4. Conclusions

Two highly galactosyl-substituted galactomannans, isolated from alfalfa and fenugreek seeds, were assessed for their cryotropic gel-forming capacity. The cryogenic processing of galactomannan solutions resulted in the formation of cryogels with diversified microstructural and mechanical aspects. The elastic modulus of the cryogels was maximized after 6 to 8 freeze-thaw cycles, where each cryogenic processing step lasted for 15 min. Although weak gels were obtained at concentrations close to the critical coil overlap concentration of the galactomannan, i.e. $c > 0.25\%$ wt, the cryostructuration was satisfactory when solutions containing at least 1 to 1.5% wt of galactomannan were subjected to cryogenic processing. Both galactomannans shared similar cryostructuring patterns, i.e. the formation of filamentous aggregates ($c < 1\%$ wt), a cellular-like gel network structure ($1 < c < 4\%$ wt) and homogeneous swollen gel-like structure ($c \geq 4\%$ wt). Alfalfa gum-based cryogels had higher elasticity and macropore interconnectivity than fenugreek ones, which was ascribed to the better ability of the former to undergo self-association via hydrogen bonding. Although the gel macropore mean size was reduced proportionally to the galactomannan content, the macropore uniformity in the fenugreek cryogels was lower, due to its ability to influence the colligative properties (ice fusion enthalpy and temperature point) of the biopolymer solutions via hydrogen bond interactions with water molecules. The physical blending of alfalfa or fenugreek gum with locust bean gum led to partial biopolymer miscibility due to excluded volume effects. However, when the microphase-separated galactomannan solutions were subject to cryogenic processing, synergistic cryostructuring effects were observed. The formation of elastically active junction zones between galactomannans highly substituted with galactose and locust bean gum was maximized at a ratio of 1:3, but it remained high for the entire range tested. Alfalfa gum cryogel synergism with locust bean gum was better than fenugreek, which was attributed to its lower water affinity and higher M/G ratio giving rise to both hydrogen bonds and hydrophobic supramolecular interactions between the polymeric aggregate clusters. Further investigation of the mechanisms of the physical interactions involved in the cryogenic processing of mixed galactomannan aqueous systems is required.

CRediT authorship contribution statement

Thierry Hellebois: Conceptualization, Investigation, Formal analysis, Writing – original draft, Writing – review & editing, Supervision. **Claire Gaiani:** Writing – review & editing, Project administration, Supervision. **Jennyfer Fortuin:** Investigation, Formal analysis, Writing – review & editing, Supervision. **Alexander Shaplov:** Investigation, Writing – review & editing. **Christos Soukoulis:** Conceptualization, Writing – review & editing, Supervision, Project administration, Funding acquisition.

Acknowledgements

This work was supported by the Luxembourg Fonds National de la Recherche (Project PROCEED: CORE/2018/SR/12675439).

Appendix A. Supplementary data

Supplementary data to this article can be found online at https://doi.org/10.1016/j.carbpol.2021.118190.

References

Balaji, P., Murugadas, A., Shanmugaapriya, S., & Abdulkader Akbarsha, M. (2019). Fabrication and characterization of egg white cryogel scaffold for three-dimensional (3D) cell culture. *Biocatalysis and Agricultural Biotechnology, 17*, 441–446. https://doi.org/10.1016/j.bcab.2018.12.019

Baudron, V., Gurikov, P., Smirnova, I., & Whitehouse, S. (2019). Porous starch materials via supercritical- and freeze-drying. *Gels, 5*(1), 12. https://doi.org/10.3390/gels5010012

Dea, I. C. M., Morris, E. R., Rees, D. A., Welsh, E. J., Barnes, H. A., & Price, J. (1977). Associations of like and unlike polysaccharides: Mechanism and specificity in galactomannans, interacting bacterial polysaccharides, and related systems. *Carbohydrate Research, 57*, 249–272. https://doi.org/10.1016/S0008-6215(00)81935-7

Doyle, J. P., Giannouli, P., Martin, E. J., Brooks, M., & Morris, E. R. (2006). Effect of sugars, galactose content and chainlength on freeze–thaw gelation of galactomannans. *Carbohydrate Polymers, 64*(3), 391–401. https://doi.org/10.1016/j.carbpol.2005.12.019

Doyle, J. P., Lyons, G., & Morris, E. R. (2009). New proposals on "hyperentanglement" of galactomannans: Solution viscosity of fenugreek gum under neutral and alkaline conditions. *Food Hydrocolloids, 23*(6), 1501–1510. https://doi.org/10.1016/j.foodhyd.2008.09.007

Ertürk, G., & Mattiasson, B. (2014). Cryogels-versatile tools in bioseparation. *Journal of Chromatography A, 1357*, 24–35. https://doi.org/10.1016/j.chroma.2014.05.055

Galante, Y. M., Merlini, L., Silvetti, T., Campia, P., Rossi, B., Viani, F., & Brasca, M. (2018). Enzyme oxidation of plant galactomannans yielding biomaterials with novel properties and applications, including as delivery systems. *Applied Microbiology and Biotechnology, 102*(11), 4687–4702. https://doi.org/10.1007/s00253-018-9028-z

Giannouli, P., & Morris, E. R. (2003). Cryogelation of xanthan. *Food Hydrocolloids, 17*(4), 495–501. https://doi.org/10.1016/S0268-005X(03)00019-5

Gillet, S., Aguedo, M., Petrut, R., Olive, G., Anastas, P., Blecker, C., & Richel, A. (2017). Structure impact of two galactomannan fractions on their viscosity properties in dilute solution, unperturbed state and gel state. *International Journal of Biological Macromolecules, 96*, 550–559. https://doi.org/10.1016/j.ijbiomac.2016.12.057

Hagiwara, T., & Hartel, R. W. (1996). Effect of sweetener, stabilizer, and storage temperature on ice recrystallization in ice cream. *Journal of Dairy Science, 79*(5), 735–744. https://doi.org/10.3168/jds.S0022-0302(96)76420-2

Hartel, R. W. (2001). Crystallization in foods. Springer US https://www.springer.com/gp/book/9780834216341.

Hellebois, T., Gaiani, C., Planchon, S., Renaut, J., & Soukoulis, C. (2021). Impact of heat treatment on the acid induced gelation of brewers' spent grain protein isolate. *Food Hydrocolloids, 113*, 106531. https://doi.org/10.1016/j.foodhyd.2020.106531

Hellebois, T., Soukoulis, C., Xu, X., Hausman, J.-F., Shaplov, A., Taoukis, P. S., & Gaiani, C. (2021). Structure conformational and rheological characterisation of alfalfa seed (Medicago sativa L.) galactomannan. Carbohydrate Polymers, 256, 117394. https://doi.org/10.1016/j.carbpol.2020.117394.

Imre, B., & Pukánszky, B. (2013). Compatibilization in bio-based and biodegradable polymer blends. *European Polymer Journal, 49*(6), 1215–1233. https://doi.org/10.1016/j.eurpolymj.2013.01.019

Kirsebom, H., Mattiasson, B., & Galaev, I. Y. (2009). Building macroporous materials from microgels and microbes via one-step cryogelation. *Langmuir, 25*(15), 8462–8465. https://doi.org/10.1021/la9006857

Kolosova, O. Y., Kurochkin, I. N., Kurochkin, I. I., & Lozinsky, V. I. (2018). Cryostructuring of polymeric systems. 48. Influence of organic chaotropes and kosmotropes on the cryotropic gel-formation of aqueous poly(vinyl alcohol) solutions. *European Polymer Journal, 102*, 169–177. https://doi.org/10.1016/j.eurpolymj.2018.03.010

Kontogiorgos, V. (2019). Galactomannans (guar, locust bean, fenugreek, tara). In L. Melton, F. Shahidi, & P. Varelis (Eds.), *Encyclopedia of food chemistry (pp. 109–113)*. Academic Press. https://doi.org/10.1016/B978-0-08-100596-5.21589-8.

Lazaridou, A., & Biliaderis, C. G. (2004). Cryogelation of cereal β-glucans: Structure and molecular size effects. *Food Hydrocolloids, 18*(6), 933–947. https://doi.org/10.1016/j.foodhyd.2004.03.003

Lazaridou, A., & Biliaderis, C. G. (2007). Cryogelation phenomena in mixed skim milk powder – Barley β-glucan–polyol aqueous dispersions. *Food Research International, 40*(7), 793–802. https://doi.org/10.1016/j.foodres.2007.01.016

Lozinsky, V. I. (2018). Cryostructuring of polymeric systems. 50.† cryogels and cryotropic gel-formation: Terms and definitions. Gels, 4(3), 77. https://doi.org/10.3390/gels4030077.

Lozinsky, V. I., Damshkaln, L. G., Brown, R., & Norton, I. T. (2000a). Study of cryostructuration of polymer systems. XVIII. Freeze–thaw influence on water-solubilized artificial mixtures of amylopectin and amylose. *Journal of Applied Polymer Science, 78*(2), 371–381. https://doi.org/10.1002/1097-4628(20001010)78:2<371::AID-APP170>3.0.CO;2-B

Lozinsky, V. I., Damshkaln, L. G., Brown, R., & Norton, I. T. (2000b). Study of cryostructuring of polymer systems. XIX. On the nature of intermolecular links in the cryogels of locust bean gum. *Polymer International, 49*(11), 1434–1443. https://doi.org/10.1002/1097-0126(200011)49:11<1434::AID-PI525>3.0.CO;2-F

Lozinsky, V. I., & Okay, O. (2014). Basic principles of cryotropic gelation. In O. Okay (Ed.), *Polymeric cryogels: Macroporous gels with remarkable properties (pp. 49–101)*. Springer International Publishing. https://doi.org/10.1007/978-3-319-05846-7_2.

Mezger, T. (2014). *The rheology handbook: For users of rotational and oscillatory rheometers* (4th ed.) Vincentz Network.

Nakagawa, K., & Nishimoto, N. (2011). Cryotropic gel formation for food nutrients encapsulation - A controllable processing of hydrogel by freezing. *Procedia Food Science, 1*, 1968–1972. https://doi.org/10.1016/j.profoo.2011.09.289

Nicolai, T. (2019). Gelation of food protein-protein mixtures. *Advances in Colloid and Interface Science*. https://doi.org/10.1016/j.cis.2019.06.006

Patmore, J. V., Goff, H. D., & Fernandes, S. (2003). Cryo-gelation of galactomannans in ice cream model systems. *Food Hydrocolloids, 17*(2), 161–169. https://doi.org/10.1016/S0268-005X(02)00048-6

Regand, A., & Goff, H. D. (2002). Effect of biopolymers on structure and ice recrystallization in dynamically frozen ice cream model systems. *Journal of Dairy Science, 85*(11), 2722–2732. https://doi.org/10.3168/jds.S0022-0302(02)74359-2

Saylan, Y., & Denizli, A. (2019). Supermacroporous composite cryogels in biomedical applications. *Gels, 5*(2), 20. https://doi.org/10.3390/gels5020020

Soukoulis, C., & Hellebois, T. (2020). *Method of extraction of galactomannan gum from alfalfa seeds*, Article PT07208LU.

Sun, H., Zhang, M., Liu, Y., Wang, Y., Chen, Y., Guan, W., … Wang, Y. (2021). Improved viability of Lactobacillus plantarum embedded in whey protein concentrate/pullulan/trehalose hydrogel during freeze drying. *Carbohydrate Polymers*. , Article 117843. https://doi.org/10.1016/j.carbpol.2021.117843

Tanaka, R., Hatakeyama, T., & Hatakeyama, H. (1998). Formation of locust bean gum hydrogel by freezing–thawing. *Polymer International, 45*(1), 118–126. https://doi.org/10.1002/(SICI)1097-0126(199801)45:1<118::AID-PI908>3.0.CO;2-T

Tolstoguzov, V. (2008). Food polymers. In J. M. Aguilera, & P. J. Lillford (Eds.), *Food materials science: Principles and practice (pp. 21–44)*. Springer. https://doi.org/10.1007/978-0-387-71947-4_3.

Zou, F., & Budtova, T. (2020). Tailoring the morphology and properties of starch aerogels and cryogels via starch source and process parameter. *Carbohydrate Polymers*. , Article 117344. https://doi.org/10.1016/j.carbpol.2020.117344